

1 **Universal continuous severity traits underlying hundreds of Parkinson's**
2 **disease clinical features**

3

4 Cynthia Sandor DMV,PhD^{1†}, Stephanie Millin DPhil^{2†}, Andrew Dahl DPhil³, Michael
5 Lawton PhD⁴, Leon Hubbard PhD⁵, Bobby Bojovic MS³, Marine Peyret-Guzzon PhD³,
6 Hannah Matten MS³, Christine Blancher PhD³, Nigel Williams PhD⁵, Yoav Ben-Shlomo
7 PhD⁴, Michele T. Hu MD, PhD^{6,7}, Donald G. Grosset MD, PhD⁸, Jonathan Marchini PhD^{3,9,*},
8 Caleb Webber PhD^{1,2,*}

9

10 **Affiliations:**

11 ¹UK Dementia Research Institute, Cardiff University, Cardiff, UK

12 ²Department of Physiology, Anatomy and Genetics, University of Oxford, Oxford, UK

13 ³Wellcome Centre for Human Genetics, University of Oxford, Oxford, UK

14 ⁴School of Social and Community Medicine, University of Bristol, Bristol, UK

15 ⁵MRC Centre for Neuropsychiatric Genetics and Genomics, Institute of Psychological
16 Medicine and Clinical Neurosciences, School of Medicine, Cardiff University, Cardiff, UK

17 ⁶Oxford Parkinson's Disease Centre, Department of Physiology, Anatomy and Genetics, Le
18 Gros Clark Building, University of Oxford, Oxford, UK

19 ⁷Nuffield Department of Clinical Neurosciences, Division of Clinical Neurology, University
20 of Oxford, Oxford, UK.

21 ⁸Department of Neurology, Institute of Neurological Sciences, Queen Elizabeth University
22 Hospital, Glasgow, United Kingdom

1 ⁹Department of Statistics, University of Oxford, Oxford, UK

2

3 *To whom correspondence should be addressed: E-mail: webberc4@cardiff.ac.uk &

4 marchini@stats.ox.ac.uk

5 †Both authors contributed equally to this work.

6

1 **Abstract**

2 The generation of deeply phenotyped patient cohorts offers an enormous potential to identify
3 disease subtypes with prognostic and therapeutic utility. Here, we quantify diverse
4 Parkinson's disease patient phenotypes on continuous scales by identifying the underlying
5 axes of phenotypic variation using a Bayesian multiple phenotype mixed model that
6 incorporates genotypic relationships. This approach overcomes many of the limitations
7 associated with clustering methods and better reflects the more continuous phenotypic
8 variation observed amongst patients. We identify three principal axes of Parkinson's disease
9 patient phenotypic variation which are reproducibly found across three independent, deeply
10 and diversely phenotyped UK and US Parkinson's disease cohorts. These three axes explain
11 over 75% of the observed clinical variation and remain robustly captured with a fraction of
12 the clinically-recorded features. Using these axes as quantitative traits, we identify significant
13 overlaps in the genetic risk associated with each axis and other human complex diseases,
14 namely coronary artery disease and schizophrenia, providing new avenues for disease-
15 modifying therapies. Our study demonstrates how deeply phenotyped cohorts can be used to
16 identify latent heritable disease-modifying traits.

17

18

1 **Introduction**

2 A critical challenge in medicine is to understand why the clinical presentations of
3 each patient affected by the same disorder vary. This is especially true for Parkinson's disease
4 (PD), for which the age of onset, the rate of progression, type and severity of symptoms differ
5 across more than a million people worldwide living with this disease ¹. To accelerate the
6 identification of disease subtypes, large deeply phenotyped cohorts of PD patients have been
7 created, in which valuable clinical, imaging, biosample and genetic data has been collected,
8 and increasingly with longitudinal monitoring ²⁻⁴.

9 Recent studies exploiting these deeply phenotyped cohorts have classified patients
10 into discrete phenotypic subgroups, each displaying a characteristic set of symptoms ⁵⁻⁷. To
11 define PD subtypes, most of these studies employ some form of variable selection to create a
12 distance matrix between individuals, followed by clustering methods such as k-means or
13 hierarchical clustering. These methods provide discrete phenotypic groups, which are
14 appealing in their categorical nature but have many shortfalls. Firstly, while selection
15 methods quantify how much variance each phenotype explains, no robust method was used to
16 define a threshold for this measure above which a phenotype contributes to the distance
17 matrix. Consequently, the definition of which phenotypes are essential to group patients and
18 which are irrelevant can be somewhat arbitrary. For example, two recent studies ^{5, 8}, using the
19 same Parkinson's Progression Markers Initiative (PPMI) cohort show divergent results:
20 apathy and hallucinations were key subtype classifiers in the first study ⁸, but not in the
21 second one ⁵, because these variables were not included. Secondly, K-means clustering
22 requires the number of phenotypic groups to be prespecified, and this choice has the potential
23 to be biased towards preconceived expectations with smaller groups ignored or erroneously
24 joined with larger groups. Finally, the creation of discrete groups may not reflect the

1 possibly continuous nature of phenotypic variability and ignores the greater statistical power
2 of continuous traits.

3 To overcome these limitations, we propose here an approach focused on the
4 continuous variation of phenotypes. Rather than focusing on presence versus absence, or mild
5 versus severe phenotypes, we incorporate the whole spectrum of severity displayed across the
6 population. For this, we applied PHENIX (PHENotype Imputation eXpediated), a multiple
7 phenotype mixed model (MPMM) approach initially developed to impute missing
8 phenotypes ⁹, that can also be exploited for genetically-guided dimensionality reduction of
9 multiple traits. This approach models the phenotypes as a combination of genetic and
10 environmental factors and the genetic component is computed from the correlation matrix
11 between the individual's genetic data.

12 Applying PHENIX to the deeply phenotyped UK-based *Discovery* cohort, we identify
13 a small number of axes underlying individual PD patient phenotypic variation that explain the
14 variation in the much larger number of clinically-observed phenotypes. We demonstrate the
15 universality of these axes of phenotypic variation amongst PD patients by independently
16 deriving similar axes in each of three cohorts: UK *Tracking* cohort including 1807
17 individuals, the UK *Discovery* cohort including 842 PD patients and US PPMI cohort
18 including 439 PD patients that has a different clinical structure from the UK cohorts. We
19 show that this reproducibility is not achieved by other commonly-used dimensionality-
20 reduction methods. Finally, we demonstrate that the genetic variation influencing the most
21 explanatory phenotypic axes in PD is shared with other specific complex diseases, opening
22 new prognostic and therapeutic avenues.

23

1 **Materials and Methods**

2 **Discovery cohort**

3 We considered 842 PD cases from the *Discovery* cohort constituted of 1700 subjects,
4 including over 1000 people with Parkinson's, plus 320 healthy controls and 340 individuals
5 thought to be 'at-risk' of developing future Parkinson's. Individuals were required to have at
6 least 90% chance of PD according to UK-Parkinson's disease brain bank criteria, no
7 alternative diagnosis and disease duration less than 3.5 years. All patients have a clinical
8 assessment repeated every eighteen months and have been already described^{4,6}. Phenotype
9 data were collected for over a hundred clinical attributes, affecting autonomic, neurological
10 and motor phenotypes (**Supplementary Fig. 1**) and described in the **Supplementary Table**
11 **1.** Genotype data were generated using the Illumina HumanCoreExome-12 v1.1 and Illumina
12 InfiniumCoreExome-24 v1.1 SNP arrays.

13 **UK Tracking Parkinson's study**

14 We considered 1807 PD cases from the *Tracking* Parkinson's cohort, which was
15 already described in detail by Malek *et al.*² and was used to identify the impact of mutations
16 within glucocerebrosidase gene (*GBA*) on different PD clinicals manifestations¹⁰. Genotype
17 data were generated using the Illumina Human Core Exome array.

18 **PPMI cohort**

19 The PPMI cohort (<http://www.ppmi-info.org>) was already described in detail
20 (including PPMI protocol of recruitment and informed consent) by Marrek *et al.*¹¹. We
21 downloaded data from the PPMI database on September 2017 in compliance with the PPMI
22 Data Use Agreement. We considered 472 newly-diagnosed typical PD subjects: subjects with
23 a diagnosis of PD for two years or less and who are not taking PD medications. We used the
24 baseline (t=0) of clinical assessments, described in detail in the **Supplementary Table 2**. We

1 excluded any individual with > 5% of missing data (437 individuals included). Participants
2 have been genotyped using two genotyping arrays, ImmunoChip ¹² and NeuroX ^{13, 14}. As
3 more participants were genotyped on NeuroX array, we used the genotype data of the
4 NeuroX chip.

5 **Methods**

6 **Genotype: quality control & Imputation**

7 Quality control was carried out independently using PLINK v1.9 ¹⁵ (SI). Imputation of
8 unobserved and missing variants was carried out separately for each cohort (SI)

9 **Phenotypic axis**

10 Our continuous measures of severity are based on a multiple phenotypes mixed model
11 approach (MPMM) named PHENIX (PHENotype Imputation eXpediated) which includes
12 genetic relationships between individuals, and is designed to impute missing phenotypes ⁹.
13 To impute missing phenotypes, PHENIX reduces the variation within a cohort to a smaller
14 number of underlying factors that are then used to predict individual missing values. Here,
15 we exploit the identification of these underlying factors as providing the latent axes of patient
16 variation which underlie a larger number of clinically observed phenotypes. The outcome is
17 that the many clinical phenotypes (sometimes missing for some individuals) of each
18 individual are represented through a smaller number of underlying latent variables of
19 phenotypic variation that manifest the observed clinical phenotypes, which we name herein
20 as *phenotypic axes*.

21 PHENIX ⁹ use a Bayesian multiple-phenotype mixed model (MPMM), where the correlations
22 between clinical phenotypes (Y) are decomposed into a genetic and a residual component
23 with the following model: $Y=U+e$, where U represents the aggregate genetic contribution
24 (whole genotype) to phenotypic variance and e is idiosyncratic noise. As the estimation of

1 maximum likelihood covariance estimates can become computationally expensive with
2 increasing number of phenotypes, PHENIX uses a Bayesian low-rank matrix factorization
3 model for the genetic term U such as: $U = S\beta$, in which β is can be used to estimate the
4 genetic covariance matrix between phenotypes and S represents a matrix of latent
5 components that each follow $\sim N(0, G)$ where G is the Estimate of Relatedness Matrix from
6 genotypes. The resulting latent traits (S) are used as phenotypic axes, each representing the
7 severity of a number of non-independent clinical phenotypes. The details to run PHENIX and
8 extract the phenotypic axes are given in the **Supplemental Information**.

9

10 **Pleiotropic enrichment evaluation with others human complex traits**

11 To investigate the similarities between genetic variation that contributes to these PD
12 phenotypic axes and genetic variation that contributes to other human complex diseases or
13 traits, we used Stratified Q-Q plots to examine differential enrichment between pre-specified
14 strata of SNPs. This approach (stratified Q-Q plot) was already used in multiple studies to
15 detect polygenic overlap between different human traits ¹⁶⁻¹⁹. This method consists of
16 making a Q-Q plot with GWAS of phenotypic axes conditional on the different strength of
17 association with other human complex diseases or traits. This representation enables us to
18 detect if conditioning on a specific human trait of interest leads to stronger enrichment in one
19 of the phenotypic axes. Enrichment is depicted by a leftward deflection in the Q-Q plot and
20 reflects a shared polygenic architecture between a specific phenotypic axis and another
21 human complex trait.

22

1 **Results**

2 **Three continuous measures capture 75% of the clinical variation.**

3 Initially, we generated phenotypic axes from a cohort of 842 PD patients (*Discovery* cohort)
4 which had been genotyped and phenotypically characterised with 40 clinical assessments
5 (**Supplementary Table 1**). Each latent axis reflected a number of co-varying observed
6 clinical assessments. Among the phenotypic axes that explained more than 5%, Axes 1, 2 and
7 3 explained 39.6%, 28.7% and 6.8% of the clinical variation respectively. Together, these 3
8 top axes account for over 75% of the clinically-observed variation (**Supplementary Fig. 2**).
9 To examine whether similar phenotypic axes are obtained in different deeply phenotyped PD
10 cohorts, we derived phenotypic axes within an independent cohort of 1807 PD individuals
11 from the UK *Tracking* cohort ² that had made similar clinical observations to the *Discovery*
12 cohort. We found significant Pearson's correlation coefficients between each cohort's first
13 three phenotypic axes: Axis 1 $r=0.92$ ($p=3 \times 10^{-13}$), Axis 2 $r=0.89$ ($p=4 \times 10^{-11}$), Axis 3
14 $r=0.72$ ($p=5 \times 10^{-6}$) (**Fig. 1**). Nevertheless, a major concern was that the identification of the
15 same phenotypic axes might, at least in part, be due to the very similar structure of the
16 clinical phenotyping between the two UK cohorts. To address this, we examined the
17 independent US-based PPMI cohort consisting of 439 sporadic PD individuals that had been
18 clinically phenotyped following a substantially different protocol to the UK cohorts. After
19 deriving phenotypic axes in the PPMI cohort, we found significant similarities between the
20 first three phenotypic axes derived for both the *Discovery*-UK and PPMI-US cohorts: the
21 coefficients of determination (R^2) between three first axes across different categories of
22 clinical phenotypes from each cohort were: Axis1: 0.665 ($p=0.048$), Axis 2: 0.914 ($p=0.003$)
23 and Axis 3: 0.754 ($p=0.025$) (**Fig. 2 & Supplementary Figure 3**). These consistent
24 similarities in the axes of phenotypic variation independently derived for each of three
25 different PD cohorts demonstrates the reproducibility of these axes of phenotypic variation

1 amongst Parkinson's patients. Finally, by comparing PHENIX with other methods of
2 dimensionality reduction, specifically Principle Component Analyses (PCA),
3 Multidimensional Scaling (MDS) and Independent component analysis (ICA), only the
4 dimensions discovered by the MPMM model, PHENIX, were significantly correlated
5 between both cohorts and thus no other method was able to identify similar axes of
6 phenotypic variation across UK and US PD cohorts (**Fig. 2**).

7 **Each phenotypic axis represents a distinct set of clinical features**

8 To interpret the clinical relevance of each phenotypic axis, we examined the
9 correlation between individual clinical features and the phenotypic axes (**Table 1 & Fig. 1 &**
10 **Supplementary Figure 4**). We observed that each phenotypic axis corresponded to a subset
11 of clinical features, differing in both extents and directions of severity. Axis 1 represented
12 worsening non-tremor motor phenotypes, anxiety and depression accompanied by a decline
13 of the cognitive function (**Table 1 & Fig. 3**). Worsening anxiety and depression were also
14 features of Axis 2, in addition to increasing severity of autonomic symptoms and increasing
15 motor dysfunction. Axis 3 was associated with general motor symptom severity including
16 rigidity, bradykinesia and tremor of the whole body independently of non-motor features.
17 The contribution of different phenotypes to these axes was therefore highly variable. Specific
18 aspects of motor dysfunction were important factors in defining the majority of axes. Anxiety
19 and depression were also relatively important features, but only for axes explaining the
20 largest amounts of variation. Conversely, cognitive impairment was associated only with
21 Axis one. However, this observation must be weighted by the fact that cognitive
22 impairment/dementia are reported at a later disease stage and thus likely under-represented in
23 recently diagnosed cases.

24 Although each phenotypic axis is associated with a distinct set of clinical features,
25 they are not independent but instead strongly correlated (**Supplementary Figure 5**). We find

1 no significant relation between the phenotypic axes and principal components of genetic
2 ancestry (**Methods**) suggesting that the phenotypic axes are not biased by the population
3 structure (**Supplementary Figure 5, Supplementary Table 3**). However, as previously
4 reported, gender influences clinical symptoms ⁴ and we also observe a significant association
5 between gender and Axis 2 (**Supplementary Table 3**, $p=4.5 \times 10^{-5}$).

6 To assess to what extent the phenotypic axes might be affected by the number of clinical
7 observations, within the *Discovery* cohort we compared the phenotypic axes built on all
8 clinical features with phenotypic axes generated with incomplete sets of randomly-selected
9 clinical features. We observed a strong correlation ($r > 0.8$) between each of the two first
10 phenotypic axes built with as few as 50% of the clinical variables and their respective
11 original phenotypic axes, suggesting that these two axes are extremely robust in terms of the
12 numbers of clinical variables considered (**Supplementary Figure 6**).

13 **The integration of genetic relationships between patients improves capture of the**
14 **Parkinson's disease clinical variation and reproducibility.**

15 The PHENIX MPMM approach employed here to derive phenotypic axes exploits the
16 genetic relatedness between individuals derived from genotypic similarity to further
17 decompose random effects into kinship effects between individuals. In its original application
18 to imputing missing phenotypes, PHENIX outperforms other imputation approaches when
19 the heritability (h^2) of a phenotype increased ⁹. Similarly, when randomly removing and re-
20 imputing 10% of observed data, the quality of the imputation of PD clinical assessments was
21 in general better when considering the genetic relatedness between individuals as compared
22 to excluding this information (**Supplementary Figure 7**), suggesting that the resulting
23 phenotypic axes better capture PD heterogeneity when including genetic information.
24 Moreover, we found a higher agreement between the phenotypic axes derived by integrating

1 the genetic relationship between patients of different cohorts than when the phenotypic axes
2 were derived ignoring the genetic relationships (**Supplementary Figure 8**). Specifically, the
3 coefficient of determination reflecting the agreement between the axes derived from the
4 Discovery and those derived from the PPMI cohorts were from Axis 1 to 3: 0.665 (p=0.048),
5 0.914 (p=0.003) and 0.754 (p=0.025) when including the genetic similarity between patients
6 as compared to 0.604 (p=0.069), 0.908 (p=0.003) and 0.001 (p=0.991) without. Together,
7 these findings demonstrate that the integration of genetic relationship between patients
8 enhances the resulting phenotypic axes' ability to reproducibly capture PD clinical variation.

9 **Metanalysis of Genome Wide Association Studies with phenotypic axes as unique and
10 universal quantitative traits**

11 Each phenotypic axis provides a quantitative trait enabling the genetics underlying
12 patient variation to be studied by performing a Genome Wide Association Study (GWAS) via
13 a regression model with the covariates age, gender, and two genetic principal components (to
14 account for any underlying population substructure) in each individual cohort. As three
15 phenotypic axes were similar across each individual cohort (*Discovery*, *Tracking* and PPMI)
16 and to increase statistical power to detect an significant association, we conducted a meta-
17 analysis of each phenotypic axis genome-wide association studies using a common set of
18 4211937 variants across 3088 individuals. A significant departure from the expected
19 quantiles was observed for Axis 1 (meta-analysis combining the summary statistic of three
20 individual GWAS [*Discovery*-*Tracking*-PPMI]) (**Supplementary Figure 9**), but no variant
21 surpassed genome-wide significance (**Supplementary Figure 10**). Although we did not
22 observe a significant genome-wide association, the use of universal phenotypic axes
23 significantly unable us to conduct meta-analysis and thus to increase the statistical power to
24 identify genetic variants through their ability to align differently deeply phenotyped cohorts
25 and reduce the number of traits tested.

1 Next, we re-examined genetic associations for each of the three phenotypic axes for
2 three major PD risk genes, namely *SNCA*, *GBA* and *LRRK2*. We found a indicative local
3 association signal but however un-significant at GWA level with Phenotypic Axis 1 for a
4 variant in *SNCA*: 4: 90758437 (p-value=1.7x10⁻⁴, **Supplementary Figure 11A**) which is in
5 high LD with rs1348224 ($r^2 > 0.8$), a SNP previously associated with PD with dementia and
6 dementia with Lewy bodies ²⁰. SNP rs1348224:G allele (minor allele) had a negative effect
7 on Phenotypic Axis 1, thus a protective effect for cognitive impairment, which is consistent
8 with a protective effect for PD with dementia and dementia with Lewy bodies previously
9 reported for this locus ²⁰. We also found a indicative local association signal (p-
10 value=1.1x10⁻⁴) with Phenotypic Axis 3 for an intronic variant in *LRRK2* (**Supplementary**
11 **Figure 11B**). Both *SNCA* and *LRRK2* variants were each nominally associated with only one
12 phenotypic axis (**Supplementary Table 4**), suggesting distinct pathogenic mechanisms.

13 **Overlaps in genetic risk associated with different diseases and specific**
14 **phenotypic axes.**

15 We then examined the overlap between genetic variation that contributes to these PD
16 phenotypic axes and the genetic variation that contributes to other human complex diseases
17 or traits. If the associations of genetic variants for one trait follow a uniform null distribution
18 when mapped onto a second trait, then there is no detected association. However, pleiotropic
19 ‘enrichment’ with another human complex trait exists if there is a significant degree of
20 deflection from the expected null, visualised by a leftward shift in the Q-Q plots conditioned
21 on the ‘pleiotropic’ effect, termed Q-Q plot inflation ^{17, 21} (**Supplementary Figure 12**). For
22 the PD phenotypic axes, we found a significant overlap between the genetic predisposition to
23 coronary artery disease with Phenotypic Axis 1 (the major severity axis) (q-value= 1.8x10⁻³)
24 and between schizophrenia and Phenotypic Axis 2 (Worsening anxiety, depression and
25 autonomic symptoms but minimal motor dysfunction) (q-value= 1.8x10⁻³) (**Fig. 4**). No

1 overlap between the genetic predisposition to PD (risk of onset) and any phenotypic axis was
2 found (**Fig. 4**). Nonetheless, by examining the pleiotropic 'enrichment' for genetic variants
3 associated with PD risk and other human traits, we did find a significant overlap with the
4 genetic predisposition associated with schizophrenia and coronary artery disease, suggesting
5 different components of the genetic risk for schizophrenia and coronary artery disease affect
6 PD risk and PD phenotypic variation (**Supplementary Figure 13**). Taken together, the
7 phenotypic axes propose two distinct aetiologies in terms of the genetic contribution to PD
8 patient variation, which provide valuable traits to be considered in the design of clinical
9 trials, for assessment of care pathways and provide distinct new avenues for therapeutic
10 research.

11

12

1 Discussion

2 We propose here a novel approach to quantifying diverse patient phenotypes on a
3 continuous scale via the use of phenotype axes. This approach overcomes many of the
4 limitations associated with the clustering methods previously used to classify PD
5 heterogeneity. By applying our approach to three independent and deeply phenotyped
6 cohorts, we demonstrate the universality of these axes of phenotypic variation amongst PD
7 patients. We also showed that our axes are robustly derived when reducing the number of
8 clinical features considered and, unlike other dimensionality reduction methods, the PHENIX
9 MPMM approach is the only method tested here that is able to identify the same phenotypic
10 axes underlying PD patient variation between individuals from different cohorts. The
11 phenotypic axes have multiple applications in PD precision medicine. Here, we explored the
12 overlap between the PD axes of clinical variation and other human traits and observed
13 different genetic predispositions associated with different phenotypic axes, suggesting several
14 distinct underlying genetic aetiologies.

15 The association of Axis 1 with genetic risk for coronary artery disease suggests an
16 influence of vasculature on the PD phenotype. While we observe no overlap in the genetics
17 influencing Body Mass Index (BMI) and Axis 1 and that it was previously reported that a
18 high BMI have protective to develop PD ²², we do observe a small but significant positive
19 correlation between patient BMI and only their Axis 1 severity score (cor =0.22; p = 3.8e-06;
20 **Supplementary Figure 14**). Furthermore, we observe that patients with a history of high
21 cholesterol or a history of heart failure, stroke and/or heart attack score significantly higher
22 only on Axis 1 than those without these histories (**Supplementary Figure 15**).

23 Although a recent study highlighted no polygenic relation between the PD risk and
24 BMI ²³, it was previously reported some overlap between major risk loci for PD and

1 schizophernia²⁴. It is an attractive idea that the dopamine (DA) neurotransmitter could
2 explain the relationship between both diseases: an excess of DA in the case of schizophrenia
3 and a reduction in PD. However, as before, we found that the schizophrenia risk alleles were
4 associated with an increasing of the PD risk, contradicting the hypothesis that PD and
5 schizophrenia are two opposed, additive phenotypes and suggesting an alternative to the
6 hypothesis of the dopaminergic system as common denominator²⁵. The genetic overlap for
7 our PD severity Axis 2 with schizophrenia but no genetic overlap between PD onset risk and
8 this axis suggests that there are distinct overlapping aetiologies contributing to risk and,
9 separately, to disease manifestation.

10 Our approach was able to identify representative quantitative variables that are
11 clinically relevant to previously-defined categorical PD subtypes. A number of known
12 comorbidities were represented among the phenotype axes. Anxiety and depression are
13 highly correlated in PD patients, both of which are correlated with Axes 1 and 2²⁶. Rigidity
14 and bradykinesia are also linked, possibly due to shared physiology²⁷, and varied in the same
15 direction along Axis 3. Lawton *et al.* reported five PD subgroups, by using the same
16 *Discovery* cohort but following a k-means clustering approach⁶. We examined the
17 distribution of phenotypic axis score across these five PD subgroups (**Supplementary Figure**
18 **16**) and noted that the 5th subgroup of patients, characterised by severe motor, non-motor and
19 cognitive disease, with poor psychological well-being clinical symptoms, were systematically
20 associated with high severity score for all three of our phenotypic axes. Inversely, the first PD
21 subgroup characterised by mild motor and non-motor disease (group affected by fewer
22 clinical symptoms) displayed a low severity score for our three phenotypic axes.
23 Furthermore, we observed that the individuals of subgroups 4 and 5, characterised by poor
24 psychological well-being, had high severity scores for phenotypic axis 2, the axis most
25 associated with depression and anxiety symptoms. These observations demonstrate some

1 consistency between subgroups defined with k-means and our phenotypic axis severity score.
2 The agreement of these phenotype axes with previously observed correlations provides
3 further support for underlying biological themes, but their reinterpretation as robust
4 continuous traits likely provides a better approximation of how the underlying biology
5 contributes, as opposed to a cut-off off for a phenotype. Specifically, the unimodal character
6 of the phenotypic axis distributions (**Supplementary Figure 17**) suggests here that the
7 development of continuous measures is more appropriate than clustering according to an
8 arbitrary threshold.

9 The phenotypic axes identified were robust in terms of the number of clinical features
10 considered and enable the alignment of patients from different cohorts with different clinical
11 phenotyping structures. The corollary is that Phenix did not require the variable selection
12 common in PD clustering approaches, and it can also guide clinicians in determining which
13 clinical assessments are essential to capture PD heterogeneity. Deep phenotyping is
14 burdensome to both patient and clinician and many of the measures exploited here are
15 compound scores summarising aspects of functioning. Further work identifying the
16 minimally burdensome observations that enable robust scoring of patients along these
17 phenotypic axes would facilitate their utility and adoption across the PD clinical community,
18 bringing increased power to the discovery of influencing factors. Finally, the MPMM
19 approach can be readily extended to include longitudinal data to determine the phenotypic
20 axes associated with disease progression while simultaneously dealing with missing data,
21 which is a common problem in longitudinal studies.

22 In conclusion, these universal axes have the potential to accelerate our understanding
23 of how PD presents in individual patients, providing more robust and objective quantitative
24 traits through which patients may be appropriately compared, through which the underlying

1 disease-modifying mechanism can be understood and appropriately stratified/personalised
2 therapeutic strategies and treatments can be developed.

3

4 **Acknowledgments**

5 The work was supported by the Monument Trust Discovery Award from Parkinson's UK.
6 Oxford Genomics Centre at the Wellcome Centre for Human Genetics, Oxford is Funded by
7 Wellcome Trust (grant reference 090532/Z/09/Z and MRC Hub grant G0900747 91070)
8 Samples and associated clinical data were supplied by the Oxford Parkinson's Disease Centre
9 (OPDC) study, funded by the Monument Trust Discovery Award from Parkinson's UK, a
10 charity registered in England and Wales (2581970) and in Scotland (SC037554), with the
11 support of the National Institute for Health Research (NIHR) Oxford Biomedical Research
12 Centre based at Oxford University Hospitals NHS Trust and University of Oxford, and the
13 NIHR Comprehensive Local Research Network. CW is supported by a UK DRI fellowship
14 funded by Medical Research Council (MRC), Alzheimer's Society and Alzheimer's Research
15 UK. CW and CS are supported by Computational Science Program funded by Michael J. Fox
16 Foundation. JM acknowledges funding for this work from the European Research Council
17 (ERC; grant 617306) . We thank the Oxford Genomics Centre at the Wellcome Centre for
18 Human Genetics, Oxford) for the generation genotyping data.

19

20 **Conflict of interest**

21 The authors declare that they have no competing interests.

22 **References**

23
24 1. Foltyne T, Brayne C, Barker RA. The heterogeneity of idiopathic Parkinson's
25 disease. *J Neurol* 2002; **249**(2): 138-145.
26

1 2. Malek N, Swallow DM, Grosset KA, Lawton MA, Marrinan SL, Lehn AC *et al.*
2 Tracking Parkinson's: Study Design and Baseline Patient Data. *J Parkinsons Dis*
3 2015; **5**(4): 947-959.

4

5 3. PPMI. PPMI.

6

7 4. Szewczyk-Krolikowski K, Tomlinson P, Nithi K, Wade-Martins R, Talbot K, Ben-
8 Shlomo Y *et al.* The influence of age and gender on motor and non-motor features of
9 early Parkinson's disease: initial findings from the Oxford Parkinson Disease Center
10 (OPDC) discovery cohort. *Parkinsonism Relat Disord* 2014; **20**(1): 99-105.

11

12 5. Fereshtehnejad SM, Zeighami Y, Dagher A, Postuma RB. Clinical criteria for
13 subtyping Parkinson's disease: biomarkers and longitudinal progression. *Brain* 2017;
14 **140**(7): 1959-1976.

15

16 6. Lawton M, Baig F, Rolinski M, Ruffman C, Nithi K, May MT *et al.* Parkinson's
17 Disease Subtypes in the Oxford Parkinson Disease Centre (OPDC) Discovery Cohort.
18 *J Parkinsons Dis* 2015; **5**(2): 269-279.

19

20 7. Lawton M, Ben-Shlomo Y, May MT, Baig F, Barber TR, Klein JC *et al.* Developing
21 and validating Parkinson's disease subtypes and their motor and cognitive
22 progression. *Journal of Neurology, Neurosurgery & Psychiatry* 2018.

23

24 8. Erro R, Picillo M, Vitale C, Palladino R, Amboni M, Moccia M *et al.* Clinical clusters
25 and dopaminergic dysfunction in de-novo Parkinson disease. *Parkinsonism Relat
26 Disord* 2016; **28**: 137-140.

27

28 9. Dahl A, Iotchkova V, Baud A, Johansson A, Gyllensten U, Soranzo N *et al.* A
29 multiple-phenotype imputation method for genetic studies. *Nat Genet* 2016; **48**(4):
30 466-472.

31

32 10. Malek N, Weil RS, Bresner C, Lawton MA, Grosset KA, Tan M *et al.* Features of
33 GBA-associated Parkinson's disease at presentation in the UK Tracking Parkinson's
34 study. *J Neurol Neurosurg Psychiatry* 2018.

35

36 11. Parkinson Progression Marker I. The Parkinson Progression Marker Initiative (PPMI).
37 *Prog Neurobiol* 2011; **95**(4): 629-635.

38

39 12. Parkes M, Cortes A, van Heel DA, Brown MA. Genetic insights into common
40 pathways and complex relationships among immune-mediated diseases. *Nat Rev
41 Genet* 2013; **14**(9): 661-673.

42

43 13. Nalls MA, Bras J, Hernandez DG, Keller MF, Majounie E, Renton AE *et al.* NeuroX,
44 a fast and efficient genotyping platform for investigation of neurodegenerative
45 diseases. *Neurobiol Aging* 2015; **36**(3): 1605 e1607-1612.

46

47 14. Nalls MA, Keller MF, Hernandez DG, Chen L, Stone DJ, Singleton AB *et al.* Baseline genetic associations in the Parkinson's Progression Markers Initiative
48 (PPMI). *Mov Disord* 2016; **31**(1): 79-85.

49

50

1 15. Purcell S, Neale B, Todd-Brown K, Thomas L, Ferreira MA, Bender D *et al.* PLINK: 2 a tool set for whole-genome association and population-based linkage analyses. *Am J 3 Hum Genet* 2007; **81**(3): 559-575.

4

5 16. Andreassen OA, Zuber V, Thompson WK, Schork AJ, Bettella F, Consortium P *et al.* 6 Shared common variants in prostate cancer and blood lipids. *Int J Epidemiol* 2014; 7 **43**(4): 1205-1214.

8

9 17. Andreassen OA, Djurovic S, Thompson WK, Schork AJ, Kendler KS, O'Donovan 10 MC *et al.* Improved detection of common variants associated with schizophrenia by 11 leveraging pleiotropy with cardiovascular-disease risk factors. *Am J Hum Genet* 2013; 12 **92**(2): 197-209.

13

14 18. Zuber V, Jonsson EG, Frei O, Witoelar A, Thompson WK, Schork AJ *et al.* 15 Identification of shared genetic variants between schizophrenia and lung cancer. *Sci 16 Rep* 2018; **8**(1): 674.

17

18 19. Winsvold BS, Bettella F, Witoelar A, Anttila V, Gormley P, Kurth T *et al.* Shared 20 genetic risk between migraine and coronary artery disease: A genome-wide analysis 21 of common variants. *PLoS One* 2017; **12**(9): e0185663.

22

23 20. Guella I, Evans DM, Szu-Tu C, Nosova E, Bortnick SF, Group SCS *et al.* alpha- 24 synuclein genetic variability: A biomarker for dementia in Parkinson disease. *Ann 25 Neurol* 2016; **79**(6): 991-999.

26

27 21. Andreassen OA, Thompson WK, Schork AJ, Ripke S, Mattingsdal M, Kelsoe JR *et 28 al.* Improved detection of common variants associated with schizophrenia and bipolar 29 disorder using pleiotropy-informed conditional false discovery rate. *PLoS Genet* 2013; **9**(4): e1003455.

30

31 22. Noyce AJ, Kia DA, Hemani G, Nicolas A, Price TR, De Pablo-Fernandez E *et al.* 32 Estimating the causal influence of body mass index on risk of Parkinson disease: A 33 Mendelian randomisation study. *PLoS Med* 2017; **14**(6): e1002314.

34

35 23. Brainstorm C, Anttila V, Bulik-Sullivan B, Finucane HK, Walters RK, Bras J *et al.* 36 Analysis of shared heritability in common disorders of the brain. *Science* 2018; 37 **360**(6395).

38

39 24. Nalls MA, Saad M, Noyce AJ, Keller MF, Schrag A, Bestwick JP *et al.* Genetic 40 comorbidities in Parkinson's disease. *Hum Mol Genet* 2014; **23**(3): 831-841.

41

42 25. Birtwistle J, Baldwin D. Role of dopamine in schizophrenia and Parkinson's disease. 43 *Br J Nurs* 1998; **7**(14): 832-834, 836, 838-841.

44

45 26. Menza MA, Robertson-Hoffman DE, Bonapace AS. Parkinson's disease and anxiety: 46 comorbidity with depression. *Biol Psychiatry* 1993; **34**(7): 465-470.

47

48 27. Berardelli A, Rothwell JC, Thompson PD, Hallett M. Pathophysiology of 49 bradykinesia in Parkinson's disease. *Brain* 2001; **124**(Pt 11): 2131-2146.

50

1
2

1 **Figure Legends**

2 **Fig. 1. The clinical phenotypes of two independent deeply phenotyped Parkinson's**
3 **disease cohorts identify the same phenotypic axes.** Results were consistent in two
4 independents cohorts (842 *Discovery* and 1807 *Tracking* patients). Examination of
5 these two separate Parkinson's disease cohorts, using independent derivation of the
6 phenotypic axes in each, showed significant correlations between each cohort's first
7 three axes. Correlations between the axes from each cohort are Axis 1 $r=0.92$ ($p=3 \times$
8 10-13), Axis 2 $r=0.89$ ($p=4 \times 10-11$), Axis 3 $r=0.72$ ($p=5 \times 10-6$). The correlation
9 coefficient (x-axis) between each axis derived in each cohort (blue: *Discovery* vs red:
10 *Tracking*) and each clinical observation (y-axis) is shown.

11

12 **Fig. 2. The reduced dimensions in other dimensionality reduction methods fail to align**
13 **between differently but deeply phenotyped UK and US Parkinson's disease**
14 **cohorts.** We compared the ability of different dimensionality reduction methods
15 (independent component analysis (ICA), Multidimensional scaling (MDS), Principal
16 component analysis (PCA) and phenotypic axis based on the PHENIX multiple
17 phenotype mixed model) to phenotypically align two deeply phenotyped Parkinson's
18 disease cohorts, specifically the *Discovery* (842 individuals) and PPMI (439 sporadic
19 Parkinson's disease) cohorts. The x-axis and y-axis represent the correlation
20 coefficient between each continuous variable with clinical observation associated with
21 a specific symptom category in *Discovery* and PPMI cohort respectively. Each
22 column panel and colour of points ("Axis") represents the dimension level of each
23 underlying dimension. All points on the diagonal would represent a perfect
24 phenotypic alignment of both cohorts. We examined the relationship between

1 correlation derived from both cohorts by performing a linear regression: R^2 and p
2 correspond to the coefficient of determination and the p-value respectively. Only the
3 dimensions discovered by the MPMM model, PHENIX, show a significant
4 relationship between both cohorts: MPMM phenotypic axes ($R^2=0.86$, $p=2\times 10^{-8}$),
5 MDS ($R^2=0.11$, $p=0.18$), ICA ($R^2=0.17$, $p=0.16$) and PCA ($R^2=0.31$, $p=0.06$).

6
7

8 **Fig. 3. The correlation of individual clinically-measured Parkinson's disease**
9 **phenotypes with an underlying Phenotypic Axis 1.** Modelling patient clinical
10 phenotypes as a combination of genetic and environmental factors revealed three
11 phenotypic severity axes (Fig.1), each representing a continuous pattern of variation
12 between multiple co-varying clinical phenotypes. In Axis 1 (shown), (A) clinical
13 measures relating to anxiety and depression and apathy are significantly and
14 positively correlated with an individual's score along this axis; patients with a higher
15 axis score have more severe mood and neuropsychiatric problems. (B) The severity of
16 motor phenotypes is positively correlated with this phenotypic axis; patients with a
17 higher axis score is associated with more severe motor phenotypes (C) Cognitive tests
18 were negatively correlated with this component (the patients that score high in these
19 cognitive tests have less cognitive impairments); individuals with a high score for this
20 component suffer from more severe anxiety, depression and displayed more cognitive
21 impairment and motor symptoms.

22

1

2 **Fig. 4. Each phenotypic axis displays a polygenic overlap with another distinct human**
3 **complex trait.** To identify pleiotropic enrichments for a phenotypic axis with another
4 human complex trait, we used a Q-Q plot stratified by pleiotropic effects (see
5 **Methods**). The significance of enrichment using Q-Q plots was calculated with a t-
6 test by comparing the subset represented in the Q-Q plots, specifically all SNPs with
7 low p-values in another human complex trait ($-\log_{10} p\text{-value} > 3$), against the depleted
8 category ($-\log_{10} p\text{-value} < 1$). Each bar plot panel (left to right) represents the
9 pleiotropic enrichment for each Phenotypic Axis (1 to 3) with other human complex
10 traits. The size of the bars corresponds to- \log_{10} FDR adjusted p-value associated
11 with pleiotropic enrichment test for that human trait. For clarity, the different human
12 traits have been classified by categories (colour bar and legend). The sources of
13 genome-wide association studies meta-analysis summary statistics of different human
14 complex traits are listed in the **Supplementary Table 5**.

15

1 **Table1:** Correlation between each axis and each clinical phenotypic measure

			r			
		Clinical Observation	Axis1	Axis2	Axis3	
Behavior	BDI total	Measure of the depression	+	0.60	0.60	0.01
	Leeds Anxiety Total	Measure of the anxiety	+	0.51	0.55	0.05
	Leeds Depression	Measure of the depression	+	0.51	0.62	0.00
	QUIP all	Impulsive-Compulsive Disorders	+	0.12	0.24	0.03
	UPDRS apathy	Apathy	+	0.40	0.39	0.18
	UPDRS fatigue	Fatigue	+	0.49	0.49	0.08
	UPDRS hallucinations	Hallucinations	+	0.17	0.17	-0.02
Autonomic	Constipation	Quantitative measure of constipation	+	-0.15	-0.07	0.01
	Orthostatic	Blood pressure from sitting/lying to stand up	+	0.17	-0.09	-0.06
	UPDRS constipation	Constipation	+	0.38	0.33	-0.08
	UPDRS pain	Pain	+	0.47	0.47	-0.01
Cognitive	Education years	Number of years of education	-	-0.21	-0.23	0.16
	MMSE total	Measure of cognitive ability	-	-0.27	-0.07	0.17
	MOCA total	Measure of cognitive ability	-	-0.31	-0.06	0.23
	Phonemic fluency	Number of words beginning with a particular letter	-	-0.26	0.03	0.14
	Semantic fluency	Number of animals and the number of boy names	-	-0.28	0.09	0.15
	BMI	Body Mass index	+	0.16	0.09	-0.08
	CGIC	Clinical global impression of change	+	0.05	-0.07	0.08
Motors	Disease Duration	Disease Duration	+	0.24	0.19	-0.07
	Flamingo time	Time that a person can stand on one leg	-	-0.46	-0.03	0.16
		Time taken for an individual to get up from a chair, walk three meters,				
	Getgo average	turn around, walk back to the chair and sit down.	+	0.52	0.04	-0.16
	Purdue assembly	Test to measure manual dexterity	-	-0.37	0.16	0.10
	Purdue total	Test to measure manual dexterity	-	-0.41	0.18	0.09
	UPDRS arms	Arms	+	0.63	-0.50	0.78
	UPDRS bradykinesia	Bradykinesia	+	0.63	-0.40	0.57
	UPDRS faceneck	Face/neck problems	+	0.26	-0.22	0.12
	UPDRS I	Non Motor Aspects of Experiences of Daily Living	+	0.68	0.67	0.02
	UPDRS II	Motor Aspects of Experiences of Daily Living	+	0.76	0.30	0.05
	UPDRS III	Motors Examination	+	0.71	-0.46	0.61
	UPDRS IV	Motors complications	+	0.16	0.16	0.05
	UPDRS laterality	Unilateral	+	-0.03	-0.01	0.15
Sensory	UPDRS legs	Legs	+	0.59	-0.31	0.44
	UPDRS postural	Postural	+	0.64	-0.02	-0.09
	UPDRS rigidity	Rigidity	+	0.51	-0.27	0.35

			+	0.22	-0.07	-0.04
	UPDRS speech	Speech	+	0.22	-0.07	-0.04
Sleep	UPDRS tremor	Tremor	+	0.20	-0.40	0.58
	ESS total	Measure of daytime sleepiness	+	0.31	0.22	-0.07
Sleep	RBD total	Measure of REM Sleep behavior disorder	+	0.29	0.29	-0.03
	Sniff total	Smell identifications	-	0.01	0.06	0.12
Drug	LEDD total	Quantitative measure of the amount of Parkinson's disease medication	+	0.31	0.27	-0.22

12

13

(1) A high score for a clinical measure indicates **more** (+) or **less** (-) issue for the patient.
 (2) The correlation coefficient under and above $|0.25|$ are indicated in gray or blue/red respectively
 (3) Red and blue cells indicates when a high phenotypic axis score are associated with more and less clinical issues for the patient respectively.

14

15

16

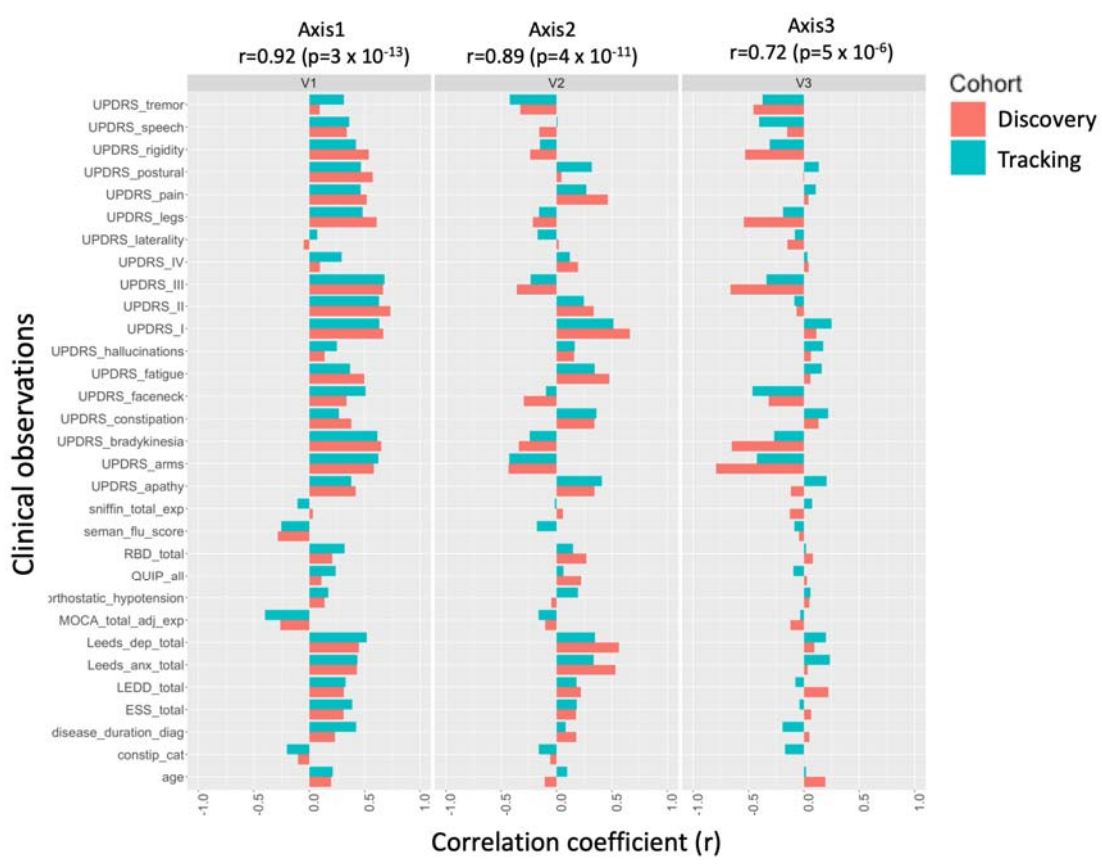
17

18

19

1 **Fig.1**

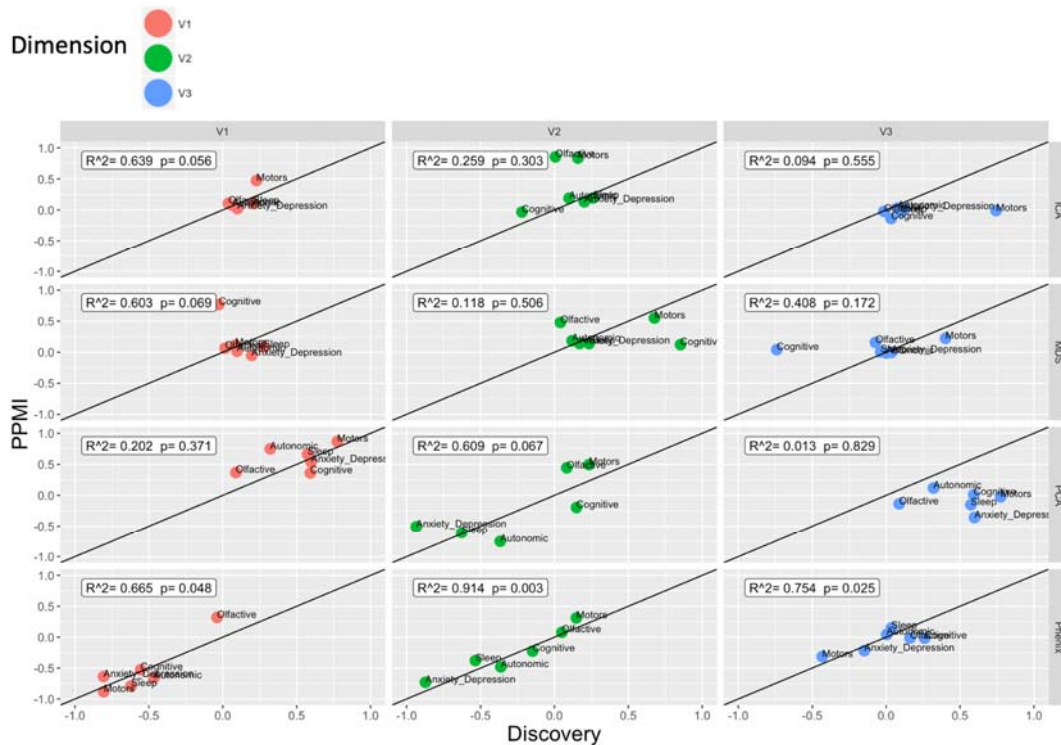
2



3

4

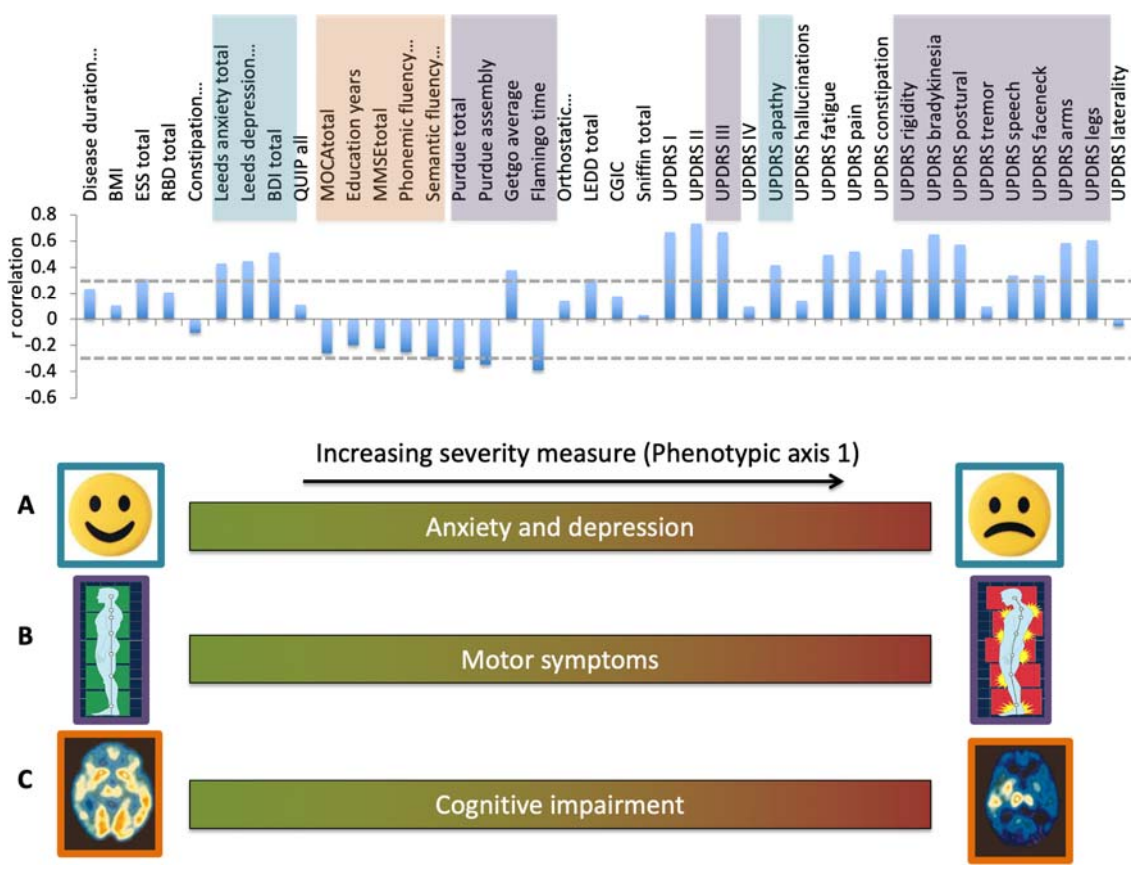
1 **Fig. 2**
2



3

1 **Fig.3**

2



1 **Fig. 4**

2

